Synchrotron-based small-angle x-ray scattering from biogenic materials

2011 Phys. Scr. 84 065802

(http://iopscience.iop.org/1402-4896/84/6/065802)

Phys. Scr. **84** (2011) 065802 (6pp) doi:10.1088/0031-8949/84/06/065802

Synchrotron-based small-angle x-ray scattering from biogenic materials

Donepudi V Rao[1], Medasani Swapna[1], Roberto Cesareo[1], Antonio Brunetti[1], Takao Akatsuka[2], Tetsuya Yuasa[2], Tohoru Takeda[3] and Giovanni E Gigante[4]

[1] Istituto di Matematica e Fisica, Universita di Sassari, Via Vienna 2, 07100 Sassari, Italy
[2] Dept of Bio-System Engineering, Faculty of Engineering, Yamagata University, 4-3-16 Jonan, Yonezawa 992-8510, Japan
[3] Institute of Clinical Medicine, University of Tsukuba, Tsukuba, Japan
[4] Departimento di Fisica, Universita di Roma 'LaSapienza', 00185 Roma, Italy

E-mail: dvrao@uniss.it

Received 25 July 2011
Accepted for publication 12 October 2011
Published 8 November 2011
Online at stacks.iop.org/PhysScr/84/065802

Abstract
We examine the small-angle x-ray scattering (SAXS) from samples of biogenic nature to study soft-matter and the associated biology. Biogenic samples are prepared from soft tissues. SAXS from different tissues varies according to both genetic (species) and environmental (habitant differences) factors. SAXS spectra (intensity versus energy (MeV)) at different Q momentum transfer values provide the crucial tool for determining the structure and enhancement of the desired property, e.g. biological activity. Fourier transform infrared (FTIR) spectroscopy was used to characterize the presence of specific chemical groups in the materials. These methods are valuable to identify various phases of calcium carbonate ($CaCO_3$). FTIR spectra were obtained in the range of wavenumbers from 4000 to 400 cm^{-1} for the external shell, soft tissue and operculum at room temperature. Finding information about the biological structures from these low-absorbing materials is one of the most important goals in the field of biological and environmental sciences and to know the mechanisms involved in bio-mineralization. These results will be utilized for the development of bio-systems.

PACS numbers: 87.85.jf, 78.70.Ck, 34.80.−i, 32.80.−t

(Some figures in this article are in colour only in the electronic version.)

1. Introduction

Small-angle x-ray scattering (SAXS) has many applications in the fields of structural biology, chemistry, physics and engineering and sample types, e.g. polymers, pharmaceuticals, cosmetics, foods, catalysts, coal, membranes and proteins. SAXS and Fourier transform infrared (FTIR) spectroscopy from biogenic samples provide a potential source of information in the field of biological and environmental sciences. These biological samples are prepared from soft tissues. We have chosen soft-bodied animals of various types with an external hard shell, e.g. the snail shell with embedded biological soft tissue. The snail shell incorporates a broader range of calcium carbonate in the biological structure. In recent years, a considerable number of studies related to these animals have been conducted in the fields of biology, paleontology, computer science, geoscience and marine geology [1]. SAXS studies and FTIR patterns from these biological samples will explore new sources of information related to bio-systems. It is interesting to study the SAXS from these soft tissues with the use of a synchrotron radiation-based intense x-ray beam and FTIR. The external shell consists of many light atoms, which are of biological importance and the embedded soft tissue linked to the soft anatomy. SAXS provides detailed analysis at nanometer length scale of the sample through the use of a micron-sized x-ray beam, which allows for greater point-to-point resolution over the sample and accurate scanning of a localized area. Obtaining information at nanometer level is valuable since each level of the structure influences the properties of a

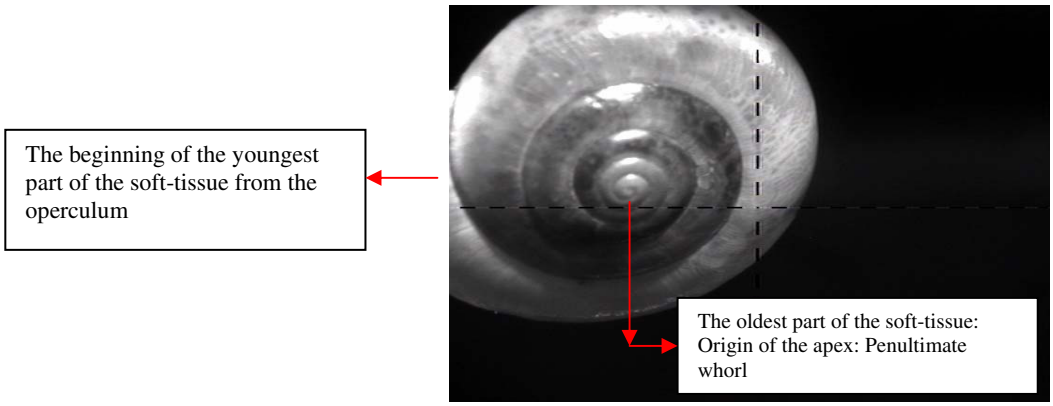

Figure 1. The physical dimension of the sample used and the prepared samples from different parts such as the external shell, soft tissue and operculum.

bio-composite. The use of synchrotron radiation permits a more intense x-ray beam, which decreases the data acquisition time [2–4].

Biological macromolecules are normally too complex to be studied directly. Yet it is possible to examine their smaller constituent molecules and to extrapolate the collected information on the molecular configuration and on the nature of the bonding in macromolecules. In this way, some important conclusions might be expected in the future with an improved physical understanding. Biological macromolecules initiate the mineralization process and are involved in the growth of minerals. In recent years, the growth of minerals in biological organisms and on bio-macromolecules extracted from these organisms and from $CaCO_3$ has received considerable attention [5, 6].

Because of the enormous x-ray fluxes available from synchrotron sources, SAXS studies on biological systems are uniquely informative; for example, biological systems will help to us solve the molecular arrangements in the sample. The experimental observable is the dynamical structure factor S (Q, Z), which describes the atomic density fluctuations spectrum. SAXS spectra (intensity versus energy (MeV)) at different Q momentum transfer values, will explore new information about the biological systems. Biological structure provides the crucial tool for determining the structure and enhancement of some desired property, for example, biological activity. SAXS uses a micro-beam allowing the ability to probe interactions between the organic and inorganic components at the nanometer level and is ideal for mapping over small areas to obtain a detailed analysis of structural variations. The origin of the embedded internal features from these biogeneic materials will be examined using a synchrotron based on SAXS and FTIR [7–11].

2. Experimental details

The x-ray source was provided by the beamline X10A at the National Synchrotron Light Source, Brookhaven National Laboratory, with a wavelength $\lambda = 1.094\,84$ Å and $E = 12.4$ keV. The magnitude of the scattering vector, $q = (4\pi/\lambda)\sin(\theta/2)$, where θ is the scattering angle. The experimental setup provided scattering angles of $0.14 < q < 2.5\,\mathrm{nm}^{-1}$ for SAXS. The data were collected by a Smart CCD camera with a 102 mm Bruker 1500 CCD camera detector.

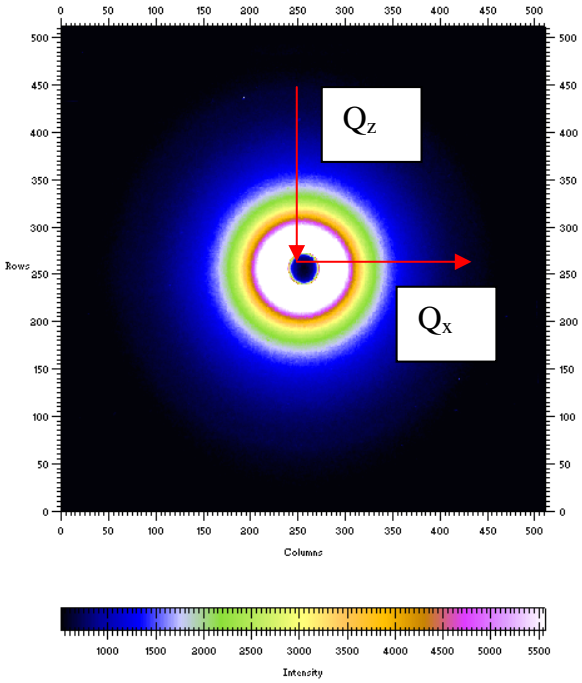

Figure 2. An SAXS 2D pattern image of the sample with a wavelength of $\lambda = 1.094\,84$ Å^{-1} and $E = 12.4$ keV. The area defined by the limits (Q_x and Q_z) indicates the area that was used to fit a Gaussian in the radial and azimuthal directions.

The distance between the samples and the detector was set at >100 cm.

2.1. FTIR spectroscopy characterization

FTIR spectroscopy was used to characterize the presence of specific chemical groups in the materials. FTIR spectra were obtained in the range of wavenumbers from 4000 to 400 cm^{-1}. The FTIR spectra were normalized and major vibration bands associated with chemical groups are reported [12].

2.2. Sample preparation

Fresh samples and soft tissues from marine 'bivalves' and 'snails' are collected in winter before spawning occurs in order to avoid the associated loss of biomass. These samples are packed in Teflon containers and stored. The soft tissue and

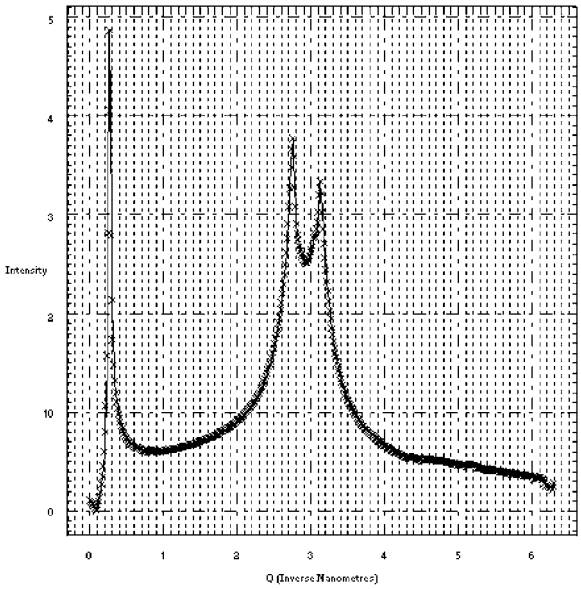

Figure 3. Variation of normalized intensity with momentum transfer without removing the body parts of the sample. The scattered peaks correspond to the external shell, soft tissue and operculum.

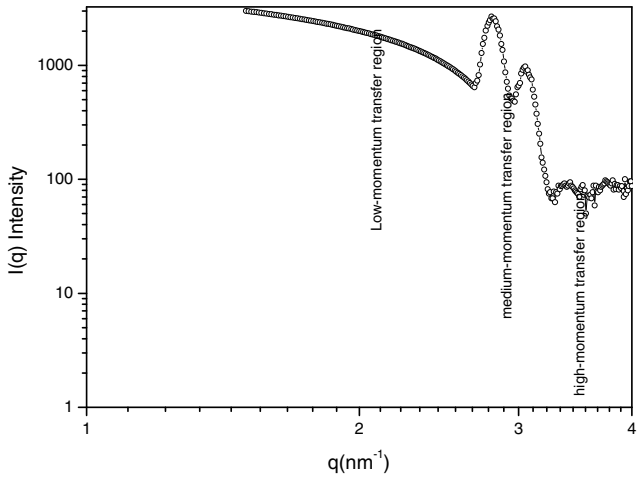

Figure 4. Variation of normalized intensity with momentum transfer mixing the body parts of the sample.

the operculum are removed from snails, cut into pieces and freeze dried. The dried samples were pulverized by a mill, and fractionated through a stainless steel sieve of 200 meshes. Approximately 5–10 mg of the sample was shaped into a pellet with a diameter of 3–5 mm and a thickness of 1–3 mm. The samples were approximately of uniform thickness, so that the scale in the SAXS patterns is the same. Samples were sandwiched between Kapton films, and this was enclosed in an airtight sample holder. This assembly was then put in the x-ray beam path, and data were collected on the samples for 30–90 min. The physical dimension of one of the samples used for imaging and for acquisition of data at the time of the experiments is shown in figure 1.

2.3. Data processing

FIT2D software and the SAXS data reduction programs were used. By means of an azimuthal integration over the

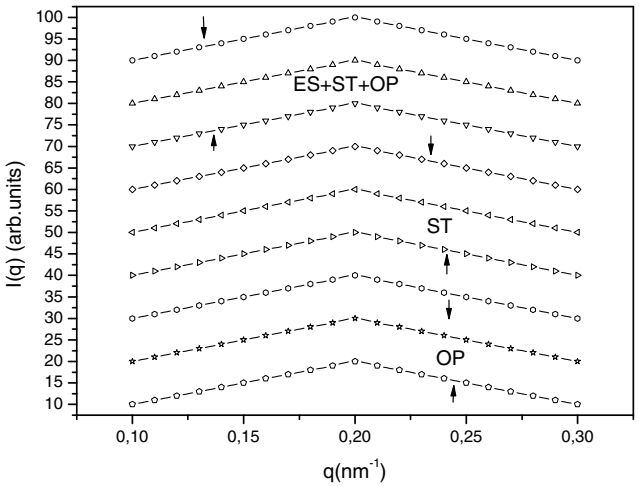

Figure 5. Normalized intensity values with momentum transfer with increasing thickness of the sample (ES + ST + OP = the external shell + soft tissue + operculum).

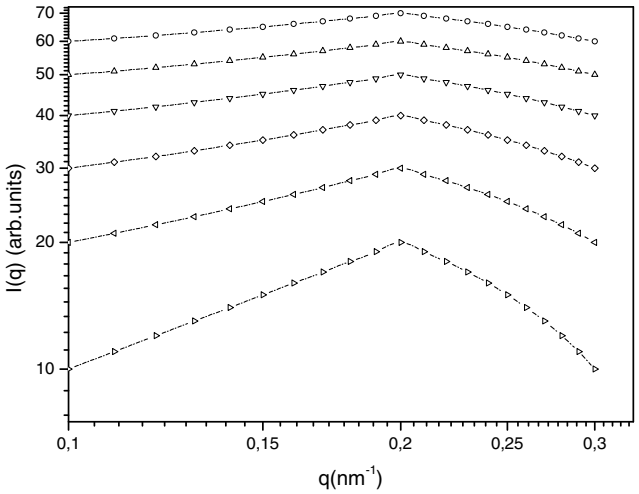

Figure 6. Normalized intensity values with momentum transfer with increasing thickness of the soft-tissue sample.

detector areas, the images are recorded to obtain scattering profiles as a function of the momentum transfer variable (q). After correction for sample transmission, scattering contribution and normalization to exposure time, it is therefore possible to produce self-consistent intensity patterns without discontinuities in the entire interval $0.04 \leqslant q \leqslant 48\,\mathrm{nm}^{-1}$.

Using FIT2D, a composite image of the two-dimensional (2D) SAXS patterns from the section scanned was compiled. The 2D SAXS patterns were spherically averaged to produce 1D linear profiles with the background subtracted. The transmission x-ray image highlights microscopic variations within the sample and is used to find regions of interest to be scanned before commencing data collection. The shell scan (figure 1) is positioned so that the soft tissue is located at the bottom of the scan and the operculum is at the top of the scan. The beam was focused at the central position of the apex, where the soft tissue begins. This also ensured that the scanning region was known for reference purposes. After taking a transmission image the whole equipment was positioned and data collection started.

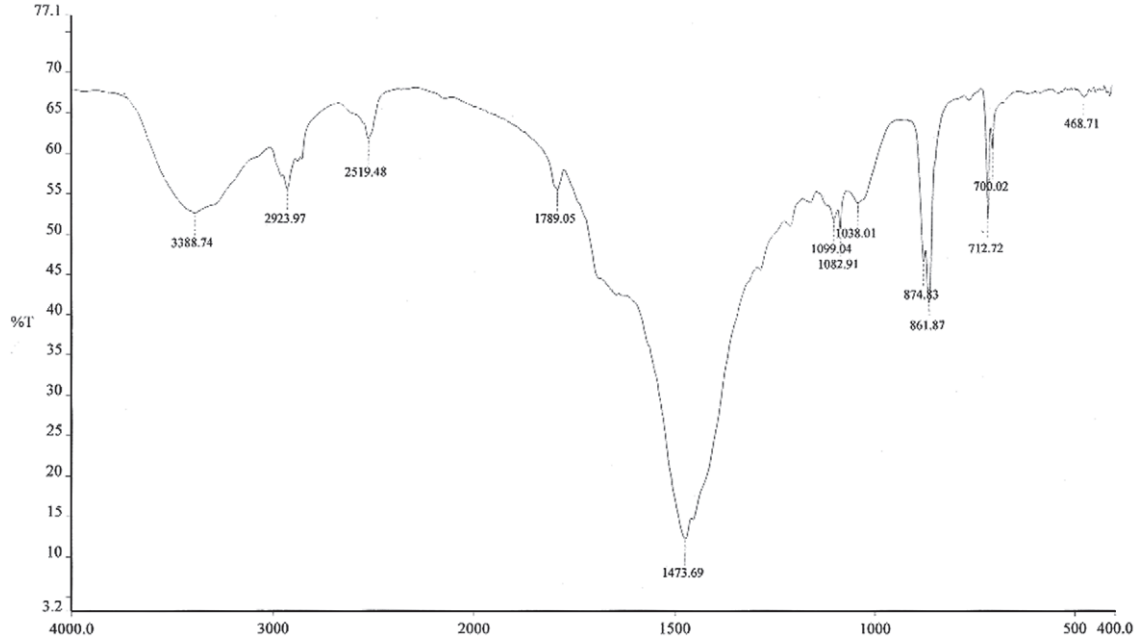

Figure 7. FTIR spectrum from the complete shell: the external shell + soft tissue + operculum.

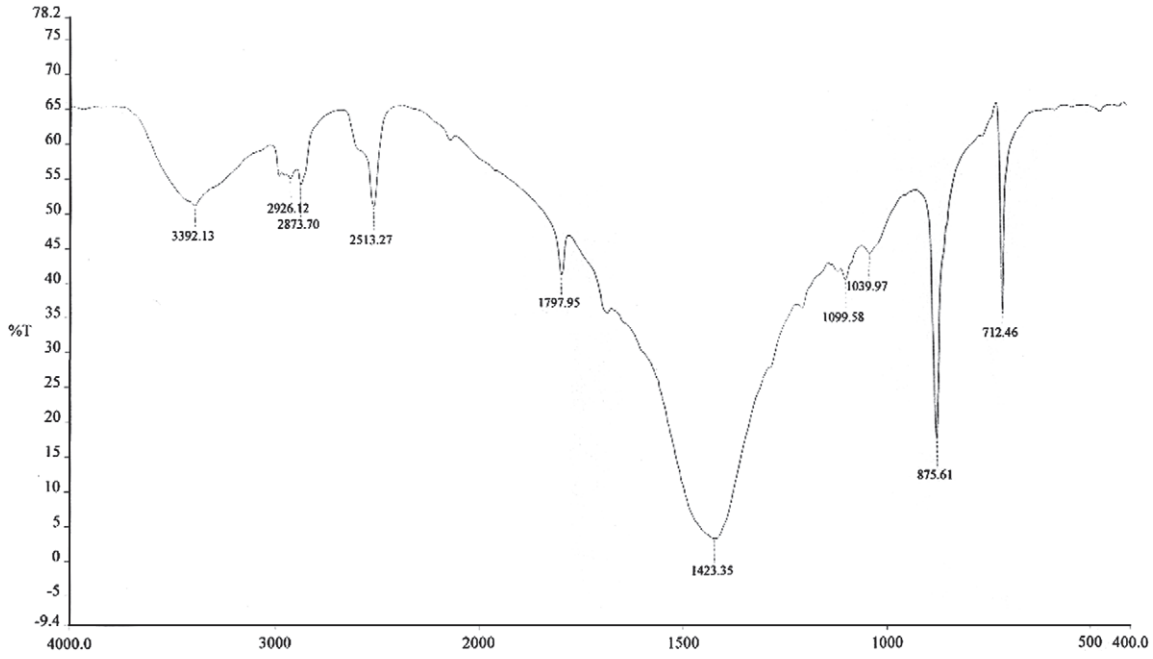

Figure 8. FTIR spectrum from the soft tissue (with the inclusion of all the body parts: the right and left pseudepipodium, head, eye, tentacles and foot).

The individual SAXS patterns had a corresponding size parameter determined for each, which were used to produce 2D maps with varying gray scale. This size parameter is calculated using the surface area to volume ratio, which can provide information on internal structural features within the material. The structure shows that there are changes in the scattering distribution within different layers of the shell.

3. Results and discussion

Data were acquired for the sample as a whole, e.g. the external shell, operculum and soft tissue for various momentum transfers. The normalized scattered intensity for each sample shows the variation of the scattered intensity for the complete sample and for the individual measured in the same manner. A 2D SAXS pattern of the image has been shown in figure 2. The area defined by the limits (Q_x and Q_z) indicates the area that was used for fitting a Gaussian in radial and azimuthal directions.

The data presented in figures 3 and 4 will be analyzed as follows. The scattered intensity from the sample as a whole (the external shell + operculum + soft tissue) will be considerably lower at high-momentum transfers. In the momentum transfer region ($0.1 \leqslant q \leqslant 10\,\mathrm{nm}^{-1}$), we observed an abrupt change. The contribution of the scattered intensity will be reduced, indicating that attenuation is confined to

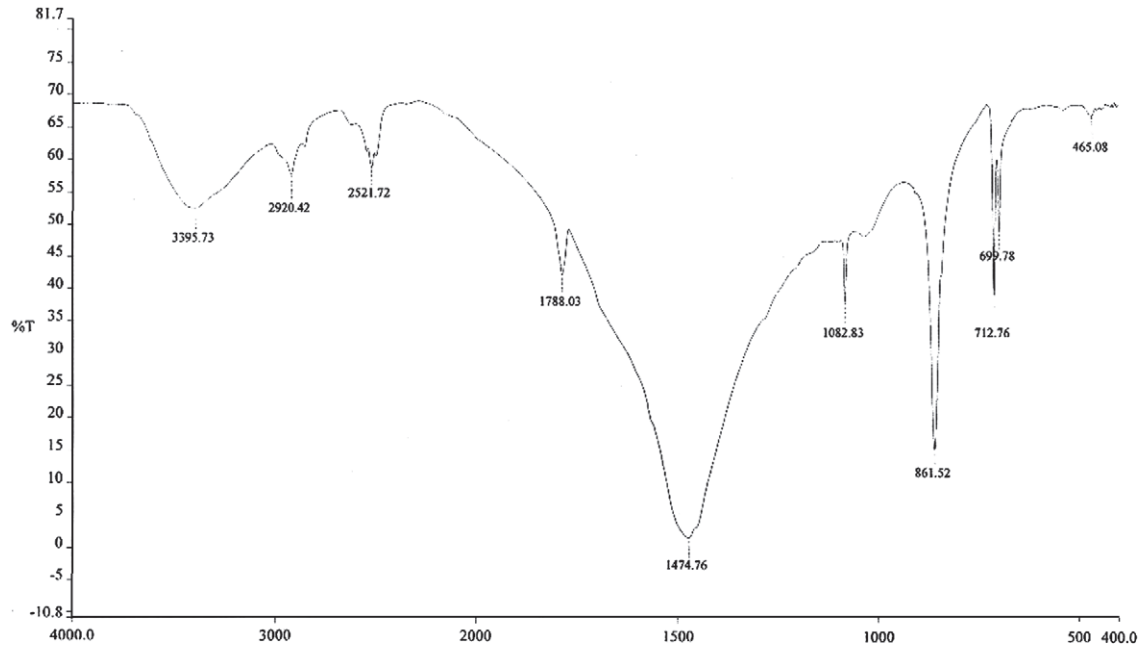

Figure 9. FTIR spectrum from the operculum.

only the hard part of the shell, i.e. pure calcium carbonate of the biological system. However, the scattered intensity will be considerably higher as the intensity traverses through the soft part of the tissue and maybe partially through the operculum in the medium-momentum transfer region ($2 \leqslant q \leqslant 32\,\mathrm{nm}^{-1}$). The contribution of the scattered intensity from the operculum will be smaller, since the amounts of calcium content will be small as distinguished from the total sample volume. However, the presence of or the accumulation of the biological trace elements may be high in the soft tissue, indicating the importance of the trace elements from these organisms and their physiological effects. The contribution of scattered intensity in the high-momentum transfer region ($4 \leqslant q \leqslant 6\,\mathrm{nm}^{-1}$) was considerably smaller. We assume that soft tissues accumulate higher metal concentrations than the shells. The external shell part is mainly composed of calcium carbonate in the form of calcite or aragonite or a mixture of both polymorphous.

The contribution of the scattered intensity from the sample as a whole (the external shell + soft tissue + operculum) with increasing thickness assessed in the medium-momentum transfer region, in order to reflect the original data acquired initially, is displayed in figure 5. Figure 6 shows the scattered intensity from the soft tissue. This medium-momentum transfer region may have a higher accumulation of minerals as distinguished from the other parts of the sample. The medium-momentum transfer region was more valuable. The analysis is shown by the 2D image presented in figure 2. The core central region is the location of the soft tissue and also the origin of the apex, where the soft tissue initially starts developing.

SAXS has been shown to be a useful tool for investigating the nucleation and growth of calcium carbonate. This type of work helps us to understand the bio-mineralization process and the conditions and factors that affect the formation, external morphology and size. This research is useful in providing information about the formation process to understand the structure of mineralized systems occurring in nature, such as the snail shell. There is little known information about the shell structure at the nanometer length scale; therefore this study has provided valuable information about the structural characteristics at this level. This study has provided valuable information on the shell at the nanometer length scale and is useful because structural information at all lengths scales, from atomic to macroscopic, is required in order to be applied to bio-inspired design of novel materials.

The FTIR spectra are shown in figures 7–9. It was observed that absorption bands of CO_3^{2-} are seen at wavenumbers of 1789.05, 1797.95, 1788.03, 1473.69, 1423.35, 1474.76, 1099.58, 1099.04, 1082.91, 1082.83, 1038.01, 1039.97, 875.61, 874.83, 861.87, 861.52, 712.76, 712.72, 712.46, 699.78, 465.08 and 468.71, which are the common feature of the CO_3^{2-} ions in $CaCO_3$. The bands in the range 875.61–861.52 can be assigned to the υ_2 (A_2) mode of CO_3^{2-}. The absorption bands in the range 1473.69–1474.76 are assigned to the υ_3 (E) mode of CO_3^{2-} ion and the absence of the IR inactive mode υ_1 (A_1). The bands in the range 3388.74, 3392.13 and 3395.73 suggest that these bands are due to the presence of water content. The bands at 1038.01 and 1039.97 correspond to the υ_1 (A_1) mode of CO_3^{2-} ions in the aragonite group. The appearance of doubly degenerate bands at 712.76, 712.72, 712.46 and 699.78 can be assigned to the υ_1 (E) mode of CO_3^{2-}. Absorption bands cantered at 874 and 712 cm^{-1} are characteristic of the calcite phase of $CaCO_3$.

Acknowledgments

DVR analyzed the results by using the facilities at ICTP, Trieste, Italy, Istituto di Matematica e Fisica, Universita di Sassari, Italy and the Department of Bio-Systems

Engineering, Yamagata University, Japan. A travel grant at the time of experiments was supported by DST, India, under the category of utilization of 'synchrotron and neutron experimental facilities'.

References

[1] Glatter O and Kratky O (ed) 1982 *Small Angle X-Ray Scattering* (London: Academic)
[2] Guinier A and Fournet G 1955 *Small Angle Scattering of X-Rays* (New York: Wiley)
[3] Lindner P 2002 *Neutrons, X-Rays and Light: Scattering Methods Applied to Soft Condensed Matter* ed P Lindner and Th Zemb (Amsterdam: Elsevier) p 23028
[4] Feigin L A and Svergun D I 1987 *Structure Analysis by Small-Angle X-Ray and Neutron Scattering* (New York: Plenum)
[5] Mann S 2001 *Biomineralization: Principles and Concepts in Bioinorganic Materials Chemistry* (New York: Oxford University Press)
[6] Veis A 2003 *Biomineralization* (*Reviews in Mineralogy and Geochemistry* vol 53) (Washington, DC: Mineralogical Society of America) p 249
[7] Hasse B, Eherenberg H, Marxen J C, Becker W and Epple M 2000 *Chem. Eur. J.* **6** 3679
[8] Pingitore N E Jr, Eastman M P, Sandidge M, Oden K and Freiha B 1988 *Mar. Chem.* **25** 107
[9] Udomkan N and Limsuwan P 2007 *Mater. Sci. Eng.* C **28** 316
[10] Aizenberg J, Lambert G, Weiner S and Addadi L 2002 *J. Chem. Soc.* **124** 32
[11] Su X, Belcher A M, Zaremba C M, Morse D E, Stucky G and Heuer A H 2002 *Chem. Mater.* **14** 3106
[12] Clark R N 1995 Reflectance spectra *Rock Physics and Phase Relations: A Handbook of Physical Constants* (*AGU Ref. Shelf* vol 3) ed T J Ahrens (Washington, DC: American Geophysical Union)